

Ca_v1.3 Channels and Intracellular Calcium Mediate Osmotic Stress-induced N-terminal c-Jun Kinase Activation and Disruption of Tight Junctions in Caco-2 Cell Monolayers*

Received for publication, March 15, 2011, and in revised form, June 23, 2011. Published, JBC Papers in Press, July 7, 2011, DOI 10.1074/jbc.M111.240358

Geetha Samak, Damodaran Narayanan, Jonathan H. Jaggar, and Radha Krishna Rao¹

From the Department of Physiology, University of Tennessee Health Science Center, Memphis, Tennessee 38163

We investigated the role of a Ca²⁺ channel and intracellular calcium concentration ([Ca²⁺]_i) in osmotic stress-induced JNK activation and tight junction disruption in Caco-2 cell monolayers. Osmotic stress-induced tight junction disruption was attenuated by 1,2-bis(2-aminophenoxy)ethane-*N,N,N',N'*-tetraacetic acid (BAPTA)-mediated intracellular Ca²⁺ depletion. Depletion of extracellular Ca²⁺ at the apical surface, but not basolateral surface, also prevented tight junction disruption. Similarly, thapsigargin-mediated endoplasmic reticulum (ER) Ca²⁺ depletion attenuated tight junction disruption. Thapsigargin or extracellular Ca²⁺ depletion partially reduced osmotic stress-induced rise in [Ca²⁺]_i, whereas thapsigargin and extracellular Ca²⁺ depletion together resulted in almost complete loss of rise in [Ca²⁺]_i. L-type Ca²⁺ channel blockers (isradipine and diltiazem) or knockdown of the Ca_v1.3 channel abrogated [Ca²⁺]_i rise and disruption of tight junction. Osmotic stress-induced JNK2 activation was abolished by BAPTA and isradipine, and partially reduced by extracellular Ca²⁺ depletion, thapsigargin, or Ca_v1.3 knockdown. Osmotic stress rapidly induced c-Src activation, which was significantly attenuated by BAPTA, isradipine, or extracellular Ca²⁺ depletion. Tight junction disruption by osmotic stress was blocked by tyrosine kinase inhibitors (genistein and PP2) or siRNA-mediated knockdown of c-Src. Osmotic stress induced a robust increase in tyrosine phosphorylation of occludin, which was attenuated by BAPTA, SP600125 (JNK inhibitor), or PP2. These results demonstrate that Ca_v1.3 and rise in [Ca²⁺]_i play a role in the mechanism of osmotic stress-induced tight junction disruption in an intestinal epithelial monolayer. [Ca²⁺]_i mediate osmotic stress-induced JNK activation and subsequent c-Src activation and tyrosine phosphorylation of tight junction proteins. Additionally, inositol 1,4,5-trisphosphate receptor-mediated release of ER Ca²⁺ also contributes to osmotic stress-induced tight junction disruption.

Epithelial tight junctions provide the barrier function that prevents the diffusion of toxins, allergens, and pathogens from external environment into the tissues and systemic circulation. Preserving the tight junction integrity, therefore, is essential for the maintenance of normal epithelial homeostasis. Various

types of stress are known to disrupt the barrier function in the gastrointestinal mucosa. Stress-induced epithelial barrier disruption plays an important role in the pathogenesis of numerous gastrointestinal diseases (1). Osmotic stress is one type of stress that the intestine faces under physiological (2) and pathophysiological conditions (3–5). Our recent study showed that osmotic stress disrupts intestinal epithelial tight junctions leading to barrier dysfunction by a JNK2 (c-Jun N-terminal kinase 2)-dependent mechanism (6). Understanding the biochemical mechanisms that underlie stress-induced cellular responses leading to disruption of epithelial tight junction and barrier function is important in developing therapeutics for the treatment of stress-related diseases.

Tight junctions are multiprotein complexes that serve as a permeability barrier, regulating the passage of ions and small molecules through a paracellular pathway. They are organized by the interactions of transmembrane proteins such as occludin, tricellulin, claudins, and junctional adhesion molecules with cytoplasmic scaffold proteins such as ZO-1, ZO-2, and ZO-3 (7). ZO-1 anchors the transmembrane proteins to the actin cytoskeleton and recruits an array of signaling proteins such as protein kinases, protein phosphatases, G proteins, etc. (8). Tight junction proteins are phosphorylated on tyrosine, serine, and threonine residues, which regulate protein-protein interactions and the integrity of tight junctions (9–12).

Calcium (Ca²⁺) is a highly versatile intracellular signaling element that can regulate numerous cellular functions and is required for the maintenance of integrity of intercellular junctional complexes. It is well established that extracellular Ca²⁺ is essential for the maintenance of intercellular junctions, including adherens junctions and tight junctions. Although it is not required for protein-protein interactions at tight junctions, extracellular Ca²⁺ is required for the maintenance of tight junction integrity. Depletion of extracellular Ca²⁺ leads to disruption of adherens junctions and tight junctions and increase in paracellular permeability in Caco-2, Madin-Darby canine kidney cells, and pulmonary and endothelial cell monolayers (13–16). Studies also indicated that the basal level of intracellular Ca²⁺ is required for the assembly of tight junctions and maintenance of its integrity (17, 18). Interestingly, a few studies showed that an increase in intracellular Ca²⁺ concentration ([Ca²⁺]_i) leads to disruption of tight junctions in endothelial monolayers (14). Therefore, the potential role of a rise in [Ca²⁺]_i and subsequent mechanisms associated with tight junction regulation are rather confusing at this point and warrants further investigation (19).

* This work was supported, in whole or in part, by National Institutes of Health Grants R01-DK55532 (to R. K. R.), R01-AA12307 (to R. K. R.), HL067061 (to J. H. J.), and HL094378 (to J. H. J.).

¹ To whom correspondence should be addressed: 894 Union Ave., Memphis, TN 38163. Tel.: 901-448-3235; Fax: 901-448-7126; E-mail: rrao2@uthsc.edu.

In the present study, we demonstrate that an elevation in $[Ca^{2+}]_i$ plays a crucial role in the mechanism of osmotic stress-induced disruption of tight junctions. We show, for the first time, that both $Ca_v1.3$ -mediated influx of extracellular Ca^{2+} and the release of ER Ca^{2+} through IP_3 -gated Ca^{2+} release channels disrupt tight junctions in an intestinal epithelial monolayer. The present study also provides evidence to indicate that $[Ca^{2+}]_i$ -induced tight junction disruption in osmotic stress-treated cell monolayers is mediated by the activation of JNK2 and c-Src-mediated tyrosine phosphorylation of tight junction proteins.

EXPERIMENTAL PROCEDURES

Chemicals—Cell culture medium (DMEM), fetal bovine serum (FBS), and antibiotics were procured from Cellgrow® (Manassas, VA). DMEM without Ca^{2+} was purchased from Invitrogen. Transfection reagents Opti-MEM®, Lipofectamine™ 2000, Oligofectamine™, and Plus™ reagents were purchased from Invitrogen. SP600125 (anthra(1,9-*cd*)pyrazol-6(2*H*)-one-1,9-pyrazoloanthron), thapsigargin, and PP2 (4-amino-5-(4-chlorophenyl)-7-(*t*-butyl)pyrazolo[3,4-*d*]pyrimidine) were purchased from Calbiochem, EMD Chemicals (San Diego, CA). BAPTA-AM, genistein, isradipine, diltiazem, and FITC-inulin were purchased from Sigma. Fura-2AM (acetoxymethyl ester) and pluronic acid were from Invitrogen. Xestospongine-C was purchased from Cayman Chemical (Ann Arbor, MI). Streptavidin-agarose was obtained from Pierce Biotechnology, Inc. and other chemicals were of analytical grade purchased from either Sigma or Fisher Scientific.

Antibodies—Rabbit polyclonal anti-JNK1/2(pTpY^{183/185}) (p-JNK) antibody was purchased from BIOSOURCE/Invitrogen. Rabbit polyclonal anti-JNK/SAPK was purchased from Upstate Biotech Inc. (Charlottesville, VA). HRP-conjugated anti-mouse IgG, HRP-conjugated anti-rabbit IgG, and anti- β -actin antibodies were obtained from Sigma. Rabbit polyclonal anti-ZO-1, rabbit polyclonal anti-occludin, and HRP-conjugated mouse monoclonal anti-occludin antibodies were purchased from Zymed Laboratories Inc.. Alexa Fluor 488-conjugated anti-mouse IgG, Cy3-conjugated anti-rabbit IgG, and Alexa Fluor 488-conjugated phalloidin were purchased from Molecular Probes (Eugene, OR). Mouse anti-GFP antibody was purchased from Clontech (Mountain view, CA). Mouse monoclonal $Ca_v1.3$ antibodies were obtained from Abcam (Cambridge, MA). Goat anti- $Ca_v1.2$ antibody was purchased from Santa Cruz Biotechnology Inc. (Santa Cruz, CA). Biotin-conjugated anti-Tyr(P) antibodies were purchased from BD Transduction Laboratories (San Jose, CA).

Antisense Oligonucleotides and siRNA—Antisense oligonucleotides for *JNK1* (AS-Jnk1) and *JNK2* (AS-Jnk2) and the

scrambled sequence for AS-Jnk1 (MS-Oligo) were designed as described previously (6) and custom synthesized in phosphorothioate form by Sigma Genosys. Human c-*SRC* and c-*YES*-specific siRNA and the corresponding control RNA were purchased from Dharmacon (Lafayette, CO).

shRNA for $Ca_v1.3$ —A vector-based short hairpin RNA (shRNA) method was used to silence $Ca_v1.3$ gene expression in Caco-2 cells. Two targeting sequences were chosen against the nucleotide sequence of human $Ca_v1.3$ (Gene ID 776 CACNA1D; NM_000720.2) using Dharmacon siDesigner software (Target 1, CCGAATAGCTCCAAGCAAA (sequence position 290–308); Target 2, GGAAGACCCAGAGATACA (sequence position 5697–5715)). The sequences were further verified by BLAST search by human genome databases, and no matches were found other than $Ca_v1.3$, confirming the uniqueness of these sequences. To construct shRNA vectors, two pairs of oligonucleotides containing the antisense sequence, hairpin loop region (TTGATATCCG), and sense sequence with cohesive BamHI and HindIII sites were synthesized (Integrated DNA Technologies Inc., Coralville, IA) as follows: top strand 1, 5'-GATCCC GCCGAATAGCTCCAAGCAAA TTGATATCCGTTTGCTTGGAGCTATTCGGTTTTTCCAAA-3' and bottom strand 1, 5'-AGCTTTTGGAAAAACCGAATAGCTCCAAGCAAAACGGATATCAATTTGCTTGGAGCTATTCGGCGG-3', top strand 2, 5-GATCCC GGAAGACCCAGAGATACATTGATATCCGTGTATCTCTGGGTCTTCCCTTTTCCAAA-3' and bottom strand 2, 5'-AGCTTTTGAAAAAGGGAAGACCCAGAGATACACGGATATCAATGTATCTCTGGGTCTTCCCGG-3'. The corresponding forward and reverse strands were annealed and inserted at BamHI and HindIII sites into pRNATin-H1.2/Neo (GenScript Corp., Piscataway, NJ) vector, which induces expression of shRNA by the H1.2 promoter and cGFP reporter gene by the cytomegalovirus promoter (Promega, WI). The constructs were transformed into DH5 α *Escherichia coli* competent cells for preparation of plasmid DNA. Plasmid DNA were isolated and purified using the Qiagen Plasmid miniprep kit (Valencia, CA). Insertion of the shRNA sequence was confirmed by releasing it by digestion with BamHI and HindIII.

Cell Culture—Caco-2 cells purchased from ATCC (Manassas, VA) were grown under standard cell culture conditions as described (20). In brief, Caco-2 cells were cultured in DMEM containing 10% (v/v) fetal bovine serum (FBS), high glucose, L-glutamine, pyruvate, and antibiotics (penicillin, streptomycin, and gentamicin). The cells were grown as monolayers in 100-mm Petri dishes or T-75 flasks. Experiments were conducted on cells grown in polycarbonate membrane transwell inserts (Costar, MA) of varying diameters (6.5, 12, and 24 mm). Studies were done on 9–11 (6.5 mm), 12–14 (12 mm), and 16–19 days (24 mm).

Transfection—Caco-2 cells grown to about 75% confluence were transfected using 1 ml of antibiotic and serum-free Opti-MEM® containing 150 nM oligonucleotides (MS-oligo, AS-Jnk1, or AS-Jnk2), c-Src siRNA, or nonspecific siRNA using 3.15 μ l of Oligofectamine reagent as described previously (6). After 24 h, the cell monolayers were trypsinized and seeded onto Transwell inserts of 6.5-, 12-, or 24-mm diameters and used for experiments on days 3 or 4 post-

² The abbreviations used are: IP_3 , inositol 1,4,5-trisphosphate; JNK, N-terminal c-Jun kinase; AS-Jnk, antisense oligonucleotide for JNK; SP600125, anthra(1,9-*cd*)pyrazol-6(2*H*)-one-1,9-pyrazoloanthron; TER, transepithelial electrical resistance; ZO, zona occludens; BAPTA-AM, 1,2-bis-(*o*-aminophenoxy)-ethane-*N,N,N',N'*-tetraacetic acid-acetoxymethyl ester; OS, osmotic stress; PP2, 4-amino-5-(4-chlorophenyl)-7-(*t*-butyl)pyrazolo[3,4-*d*]pyrimidine; CFM, Ca^{2+} -free medium; TRPV4, transient receptor potential vanilloid family Ca^{2+} channel 4; $Ca_v1.2$, $Ca_v1.3$, voltage-dependent calcium channels 1.2 and 1.3; ER, endoplasmic reticulum.

Tight Junction Regulation by Intracellular Calcium

seeding. Transfection of shRNA for *Ca_v1.3* was performed using LipofectamineTM 2000 reagent according to the manufacturer's protocol. Briefly, cells were transfected with 1 μ g of plasmid DNA (shRNA1, shRNA2, or empty vector) using Lipofectamine 2000 and Plus reagent in 50 μ l of Opti-MEM, and incubated for 30 min at room temperature. The transfection mixture was then replaced with normal DMEM containing serum and antibiotics. After 24 h, cell monolayers were trypsinized, seeded onto Transwell inserts from Costar (Cambridge, MA), and used for experiments on days 3 or 4 after seeding.

Osmotic Stress and Treatment with Inhibitors—Cell monolayers in transwells were incubated in 600 mosM DMEM (osmolarity adjusted with mannitol) in apical or basal compartment to induce osmotic stress. Barrier disruption was evaluated by measuring TER and inulin flux. SP600125 (1 μ M) or genistein (100 μ M) were administered 50 min prior to osmotic stress and PP2 (3 μ M) was administered 30 min prior to osmotic stress. For extracellular Ca^{2+} depletion, Ca^{2+} -free medium (CFM) was used to prepare the hyperosmolar medium and administered either to apical (CFM-A) or basal (CFM-B) compartments. Intracellular Ca^{2+} depletion was achieved by preloading cells with 10 μ M BAPTA-AM. Ca^{2+} channel blockers, thapsigargin (1 μ M), isradipine (1 μ M), or diltiazem (100 μ M) were administered 30 min prior to osmotic stress and 1 μ M xestospongine-C was added 15 min before osmotic stress.

Measurement of TER—TER was measured as described previously (20) using a Millicell-ERS Electrical Resistance System (Millipore, Bedford, MA). TER was calculated as $\Omega \cdot cm^2$ by multiplying it with the surface area of the monolayer. The TER of the polycarbonate membrane in Transwells ($\sim 30 \Omega \cdot cm^2$) was subtracted from all readings.

Unidirectional Flux of Inulin—Transwells with the cell monolayers were incubated under varying experimental conditions in the presence of FITC-inulin (0.5 mg/ml) in the basal well. At varying times of treatment, 50 μ l of apical medium was withdrawn and fluorescence was measured using a plate reader (BioTEK Instruments, Winooski, VT). The flux into the apical well was calculated as the percent of total fluorescence administered into the basal well per hour per cm^2 surface area.

Immunofluorescence Microscopy—Cell monolayers were fixed in 3% paraformaldehyde in PBS. Following permeabilization in 0.2% Triton X-100, cell monolayers were blocked in 4% nonfat milk in TBST (20 mM Tris, pH 7.2, and 150 mM NaCl). They were incubated for 1 h with primary antibodies (rabbit polyclonal anti-ZO-1 and mouse monoclonal anti-occludin), followed by a 1-h incubation with secondary antibodies, Alexa Fluor 488-conjugated anti-mouse IgG and Cy3-conjugated anti-rabbit IgG antibodies. The fluorescence was examined under a Zeiss LSM 5 laser scanning confocal microscope, and images from *x-y* sections (1 μ m) were collected using LSM 5 Pascal software. Images were stacked using the software, Image J (NIH), and processed by Adobe Photoshop (Adobe Systems Inc., San Jose, CA).

Intracellular Ca^{2+} Measurements—Caco-2 cell monolayers were grown on 20-mm diameter glass-bottom microwell dishes of (MatTek, Ashland, MA) for 5 days. Cells were serum starved for 12 h and washed with HBSS prior to incubation in HEPES-

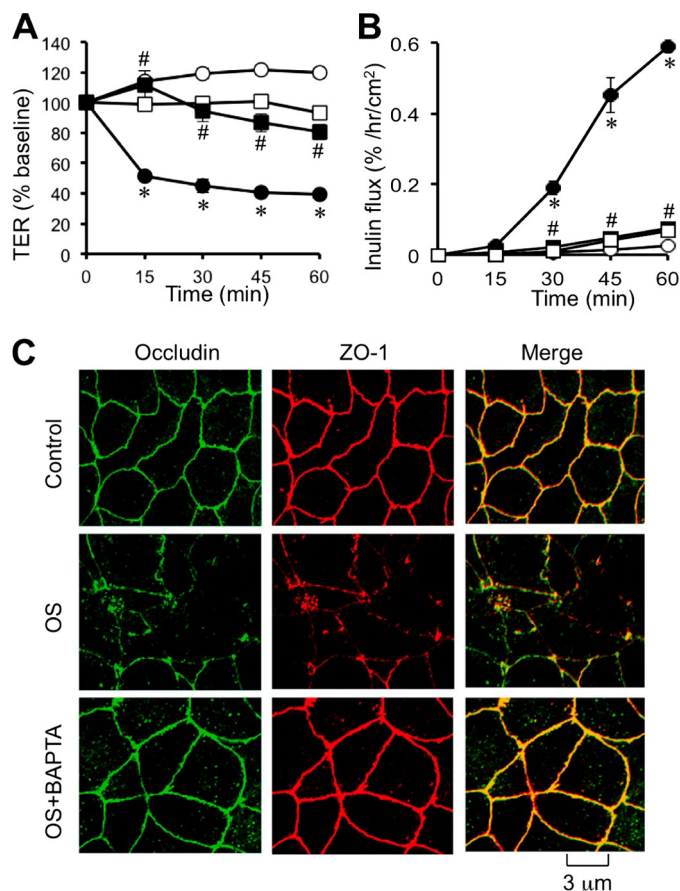


FIGURE 1. Intracellular calcium is required for osmotic stress-induced tight junction disruption. A and B, Caco-2 cell monolayers were pretreated with (□, ●) or without (○, ●) BAPTA-AM for 20 min and osmotic stress (●, ■) was induced as described under "Experimental Procedures." TER (A) and unidirectional inulin flux (B) were measured at varying times. Values are mean \pm S.E. ($n = 6$). Asterisks indicate the values that are significantly ($p < 0.05$) different from corresponding values for control group, and # indicates the values that are significantly ($p < 0.05$) different from corresponding values for osmotic stress without BAPTA. C, cell monolayers in different groups at 1 h after OS were fixed and stained for occludin and ZO-1 by the immunofluorescence method. Preloading cells with BAPTA did not cause a significant change in TER or inulin permeability.

buffered solution (134 mM NaCl, 6 mM KCl, 2 mM $CaCl_2$, 1 mM $MgCl_2$, 10 mM HEPES, and 10 mM glucose, pH 7.4) containing the fluorescent Ca^{2+} probe, Fura-2 AM (10 μ M), and 0.5% pluronic F-127 for 30 min, followed by a 15-min wash. Fura-2-loaded Caco-2 cells were alternately excited at 340 or 380 nm using a PC driven hyperswitch (Ionoptix, MA). Ratios were collected every second at 510 nm using a Dage MTI iCCD camera and Ionwizard software (Ionoptix). Intracellular Ca^{2+} concentrations were calculated using Equation 1,

$$[Ca^{2+}]_i = \frac{K_d(R - R_{min})(S_{f2})}{(R_{max} - R)(S_{b2})} \quad (\text{Eq. 1})$$

where R is the 340/380 nm ratio, R_{min} and R_{max} are the minimum and maximum ratios determined in Ca^{2+} -free and saturating Ca^{2+} solutions, respectively. S_{f2}/S_{b2} is the Ca^{2+} free/ Ca^{2+} replete-ratio of emissions at 380 nm excitation, and K_d is the dissociation constant for Fura-2. R_{min} , R_{max} , S_{f2} , and S_{b2} were determined by increasing the Ca^{2+} permeability of Caco-2 cells with ionomycin (10 mM), and perfusing cells with a

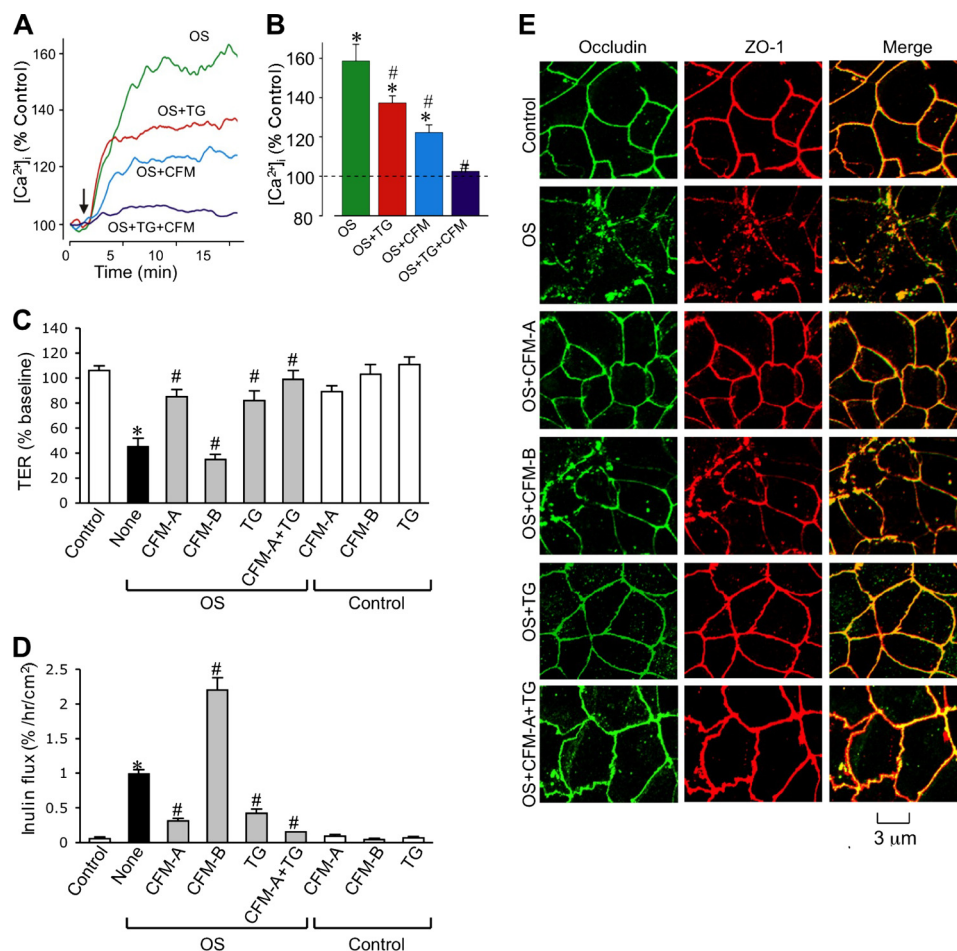


FIGURE 2. Extracellular calcium influx and intracellular store-operated calcium release are necessary for osmotic stress-induced tight junction disruption. *A* and *B*, Fura-2-loaded Caco-2 cell monolayers were exposed to OS in the presence or absence of thapsigargin (TG) and/or CFM. Real time (*A*) change in the levels of intracellular calcium was measured for up to 45 min as described under "Experimental Procedures." Steady state calcium levels are averaged (*B*); 8–10 cells in each of 3 monolayers per group were analyzed. Values are mean \pm S.E. Asterisks indicate the values that are significantly ($p < 0.05$) different from corresponding baseline values, and # indicates the values that are significantly ($p < 0.05$) different from value for OS group. *C* and *D*, Caco-2 cell monolayers were pretreated with thapsigargin or incubated with calcium-free medium in the apical compartment (CFM-A) or basal compartment (CFM-B). Osmotic stress was induced by administration of hyperosmotic medium as described under "Experimental Procedures." Control groups, with or without TG or CFM, received no osmotic stress. TER (*C*) and unidirectional inulin flux (*D*) were measured after 1 h. Values are mean \pm S.E. ($n = 6$). Asterisks indicate the values that are significantly ($p < 0.05$) different from corresponding values for the control group, and # indicates the values that are significantly ($p < 0.05$) different from corresponding values for OS without TG or CFM treatment. *E*, cell monolayers exposed to OS with or without TG and CFM were fixed at 1 h after OS and stained for occludin and ZO-1 by immunofluorescence method.

high Ca^{2+} (10 mM) or Ca^{2+} -free (10 mM EGTA) solution. The *in situ* apparent dissociation constant (K_d) for Fura-2 used in this study was 224 nM. Eight to 10 cells in each monolayer were analyzed simultaneously, and experiments were repeated in 3–5 monolayers.

Immunoprecipitation—Caco-2 cell monolayers were washed with ice-cold PBS and proteins were extracted in hot lysis buffer D (0.3% SDS in 10 mM Tris buffer, pH 7.4, containing 1 mM sodium orthovanadate, 10 mM sodium fluoride, 1 mM PMSE, and 10 $\mu\text{l/ml}$ of protease inhibitors mixture). Homogenate was heated at 100 $^{\circ}\text{C}$ for 10 min, suspended with a 25-gauge syringe 5 times, and centrifuged to collect the clear supernatant. Protein content was measured by the BCA method (Pierce). Phospho-Tyr was immunoprecipitated as described before (21) using biotin-conjugated anti-Tyr(P) antibody. Immunocomplexes were isolated by precipitation using streptavidin-agarose and immunoblotted for ZO-1 and occludin using mouse monoclonal anti-ZO-1 and HRP-conjugated mouse monoclonal anti-occludin antibodies.

Cell Lysate and Immunoblot Analysis—Proteins from the cells were extracted in heated lysis buffer D as described above (21). An aliquot was taken for protein estimation, and the lysate was mixed with equal volume of Laemmli's sample buffer (two times concentrated), heated at 100 $^{\circ}\text{C}$ for 10 min. Proteins were separated in a 7% gel using SDS-polyacrylamide gel electrophoresis and transferred to PVDF membrane. The membranes were probed for *p*-JNK, JNK 1/2, *p*-Src, $\text{Ca}_v1.2$, $\text{Ca}_v1.3$, c-Src, ZO-1, occludin, or β -actin by using a combination of the specific primary antibodies with corresponding HRP-conjugated anti-mouse IgG or HRP-conjugated anti-rabbit IgG secondary antibodies. The blot was developed using the chemiluminescence (ECL) system (Amersham Biosciences/GE Healthcare). Densitometric analysis of specific bands was done using the Image J software.

Statistical Analysis—The observed data in the two different groups was compared using Student's *t* tests for grouped data. Significance in all tests was set at 95% or greater confidence level.

Tight Junction Regulation by Intracellular Calcium

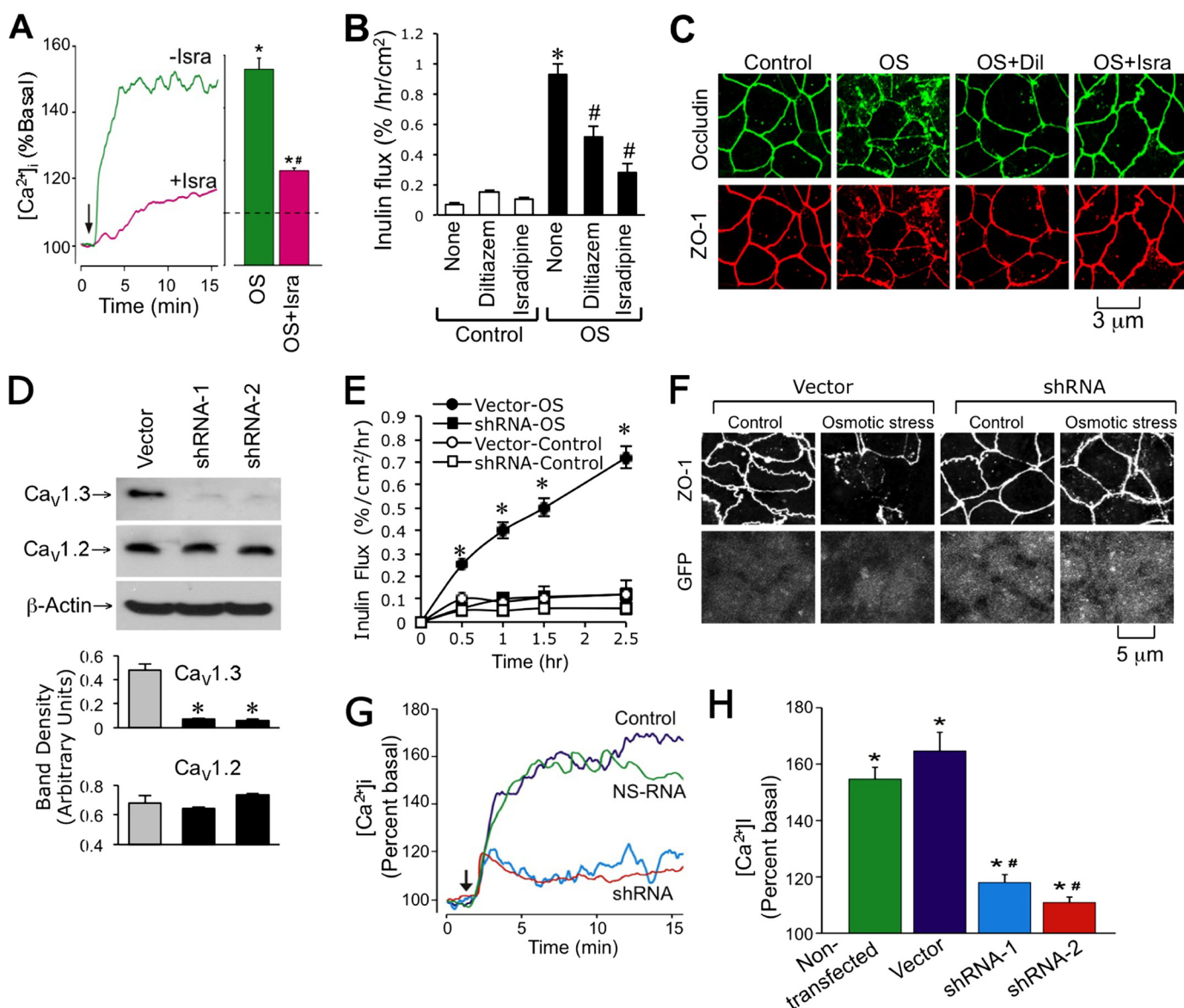


FIGURE 3. $Ca_v1.3$ mediates osmotic stress-induced calcium influx and tight junction disruption. *A*, Fura-2-loaded Caco-2 cell monolayers were exposed to OS in the presence or absence of isradipine (*Isra*). Real time (*A*) change in the levels of $[Ca^{2+}]_i$ was measured as described under "Experimental Procedures." Steady state $[Ca^{2+}]_i$ was evaluated. Asterisks indicate the values that are significantly ($p < 0.05$) different from baseline values, and # indicates the values that are significantly ($p < 0.05$) different from corresponding values for the OS group. *B*, Caco-2 cell monolayers were pretreated with or without diltiazem or isradipine for 40 min prior to incubation with or without OS. Inulin permeability was measured at 1 h after OS. Values are mean \pm S.E. ($n = 6$). Asterisks indicate the values that are significantly ($p < 0.05$) different from the corresponding values for control group, and # indicates the values that are significantly ($p < 0.05$) different from corresponding values for the "None" OS group. *C*, cell monolayers in different groups at 1 h after osmotic stress were fixed and stained for occludin and ZO-1 by the immunofluorescence method. *D*, protein extracts from Caco-2 cells transfected with the empty vector or $Ca_v1.3$ -shRNAs were immunoblotted for $Ca_v1.3$ and $Ca_v1.2$. Band densities were evaluated and the values are mean \pm S.E. ($n = 3$). Asterisks indicate the values that are significantly ($p < 0.05$) different from the corresponding value for Vector group. *E*, inulin permeability was measured during osmotic stress in monolayers of cells transfected with empty vector or $Ca_v1.3$ -shRNA. Asterisks indicate the values that are significantly ($p < 0.05$) different from corresponding values for vector-transfected cells. *F*, cell monolayers in different groups at 1 h after osmotic stress were fixed and stained for ZO-1 and GFP by the immunofluorescence method. *G* and *H*, intracellular calcium was measured during oxidative stress in vector or $Ca_v1.3$ -shRNA-transfected cell monolayers. Steady state values were evaluated and the values are mean \pm S.E. ($n = 3$). Asterisks indicate the values that are significantly ($p < 0.05$) different from corresponding baseline values, and # indicates the values that are significantly different ($p < 0.05$) from values for vector group.

RESULTS

Intracellular Ca^{2+} Is Required for Osmotic Stress-induced Tight Junction Disruption—A recent study demonstrated that osmotic stress disrupts tight junctions and induces barrier dysfunction in Caco-2 cell monolayers and mouse ileum (6). In the present study, we evaluated the effect of $[Ca^{2+}]_i$ on osmotic stress-induced tight junction disruption. Osmotic stress

reduced TER (Fig. 1*A*) and increased inulin permeability (Fig. 1*B*) in a time-dependent manner. Pretreatment of cell monolayers with BAPTA-AM (a cell permeable Ca^{2+} chelator) significantly attenuated a osmotic stress-induced decrease in TER and increase in inulin permeability. BAPTA-AM pretreatment also attenuated osmotic stress-induced redistribution of occludin and ZO-1 from the intercellular junctions into the intracel-

lular compartment (Fig. 1C). BAPTA treatment, by itself, produced no significant effect on TER, inulin permeability, or distribution of occludin and ZO-1.

Ca²⁺ Influx and ER Ca²⁺ Release Are Involved in Osmotic Stress-induced Tight Junction Disruption—The effect of osmotic stress on [Ca²⁺]_i was evaluated in Fura-2-loaded Caco-2 cell monolayers. Osmotic stress rapidly increased [Ca²⁺]_i, reaching a maximum by 15 min (Fig. 2A). Pretreatment of cell monolayers with thapsigargin (an ER Ca²⁺-ATPase inhibitor that depletes ER Ca²⁺) partially reduced the osmotic stress-induced increase in [Ca²⁺]_i. Similarly, removal of extracellular Ca²⁺ also partially reduced osmotic stress-induced [Ca²⁺]_i. Osmotic stress-induced increase in [Ca²⁺]_i was almost abolished when cells were simultaneously treated with thapsigargin and Ca²⁺-free medium (Fig. 2, A and B).

Removal of extracellular Ca²⁺ or pretreatment of cells with thapsigargin also attenuated an osmotic stress-induced decrease in TER (Fig. 2C) and increase in inulin permeability (Fig. 2D). This effect on osmotic stress-induced changes in TER and inulin permeability was significantly greater when Ca²⁺ depletion and thapsigargin treatment were applied simultaneously. Interestingly, depletion of Ca²⁺ from the apical buffer, but not from the basal buffer, was effective in preventing the osmotic stress effect on barrier function. Ca²⁺ depletion in the basolateral buffer rather exacerbated osmotic stress-induced inulin permeability (Fig. 2D). Thapsigargin treatment or removal of Ca²⁺ from apical or basal buffers did not alter TER or inulin flux in the absence of osmotic stress. Osmotic stress-induced redistribution of occludin and ZO-1 was also attenuated by thapsigargin or Ca²⁺-free medium on the apical surface (Fig. 2E). Removal of Ca²⁺ from the basal buffer failed to prevent osmotic stress-induced redistribution of occludin and ZO-1.

Ca_v1.3 Contributes to Osmotic Stress-induced Ca²⁺ Influx and Tight Junction Disruption—The requirement of extracellular Ca²⁺ in the apical compartment indicated that Ca²⁺ influx through Ca²⁺ channels on the apical membrane is involved in osmotic stress-induced barrier dysfunction. Some of the well characterized Ca²⁺ channels on the apical membrane of intestinal epithelial cells include L-type voltage-gated channels, such as Ca_v1.3 (19). Therefore, we evaluated the effect of diltiazem and isradipine (L-type Ca²⁺ channel blockers) on the osmotic stress-induced increase in [Ca²⁺]_i and disruption of barrier function. Both diltiazem and isradipine partially reduced osmotic stress-induced [Ca²⁺]_i (Fig. 3A), and significantly attenuated the osmotic stress-induced increase in inulin permeability (Fig. 3B) and redistribution of occludin and ZO-1 from the intercellular junctions (Fig. 3C).

Evidence indicates that Ca_v1.3 contributes to Ca²⁺ absorption from the apical surface (19). Therefore, we evaluated the effect of Ca_v1.3 gene silencing on osmotic stress-induced tight junction disruption. Ca_v1.3 shRNA reduced the Ca_v1.3 protein in Caco-2 cells compared with that in vector-transfected cells (Fig. 3D). In contrast, shRNA did not alter the Ca_v1.2 protein, indicating the specificity of shRNA. Knockdown of Ca_v1.3 did not alter the basal level of [Ca²⁺]_i. Knockdown of Ca_v1.3 effectively blocked the osmotic stress-induced increase in inulin permeability (Fig. 3E) and attenuated redistribution of ZO-1 from intercellular junctions (Fig. 3F). Ca_v1.3 knockdown by

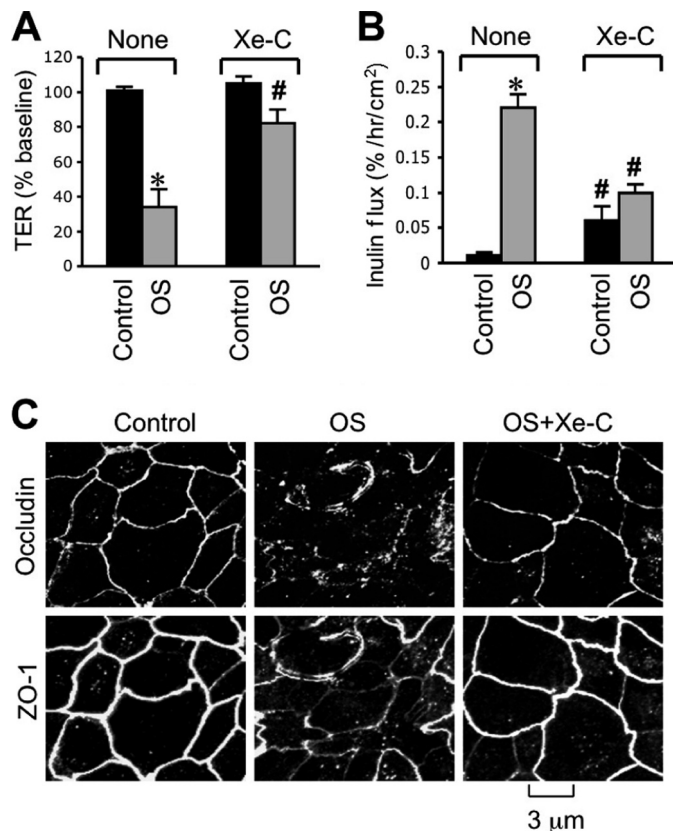


FIGURE 4. IP₃ receptor-mediated intracellular calcium release is involved in osmotic stress-induced tight junction disruption. Caco-2 cell monolayers were pretreated with or without xestospongine-C (Xe-C) for 30 min and OS was induced as described under "Experimental Procedures." TER (A) and unidirectional inulin flux (B) were measured at 1 h after osmotic stress. Values are mean ± S.E. (n = 6). Asterisks indicate the values that are significantly (p < 0.05) different from the corresponding control values, and # indicates the values that are different from values for OS without Xe-C. C, cell monolayers in different groups at 1 h after osmotic stress were fixed and stained for occludin and ZO-1 by the immunofluorescence method.

shRNA markedly reduced the osmotic stress-induced increase in [Ca²⁺]_i (Fig. 3, G and H).

IP₃ Receptor-mediated ER Ca²⁺ Release Is Involved in Osmotic Stress-induced Tight Junction Disruption—A significant reduction of the osmotic stress-induced increase in [Ca²⁺]_i by thapsigargin indicated that ER Ca²⁺ release is a partial contributor to elevated [Ca²⁺]_i. One of the mechanisms associated with ER Ca²⁺ release involves IP₃ receptor activation. Therefore, we evaluated the effect of xestospongine C (IP₃ receptor antagonist) on the osmotic stress effect. Pretreatment of cell monolayers with xestospongine C significantly attenuated the osmotic stress-induced decrease in TER (Fig. 4A) and increase in inulin permeability (Fig. 4B). Xestospongine C also prevented osmotic stress-induced redistribution of occludin and ZO-1 from intercellular junctions (Fig. 4C). Xestospongine C, by itself, showed a slight but significant increase in inulin permeability in the absence of osmotic stress.

Intracellular Ca²⁺ Mediates Osmotic Stress-induced JNK Activation—A recent study demonstrated that osmotic stress rapidly activates JNK and that osmotic stress-induced tight junction disruption is mediated by JNK2 activity (6). Therefore, we examined the potential role of [Ca²⁺]_i in osmotic stress-induced JNK activation. Results show that the osmotic stress-

Tight Junction Regulation by Intracellular Calcium

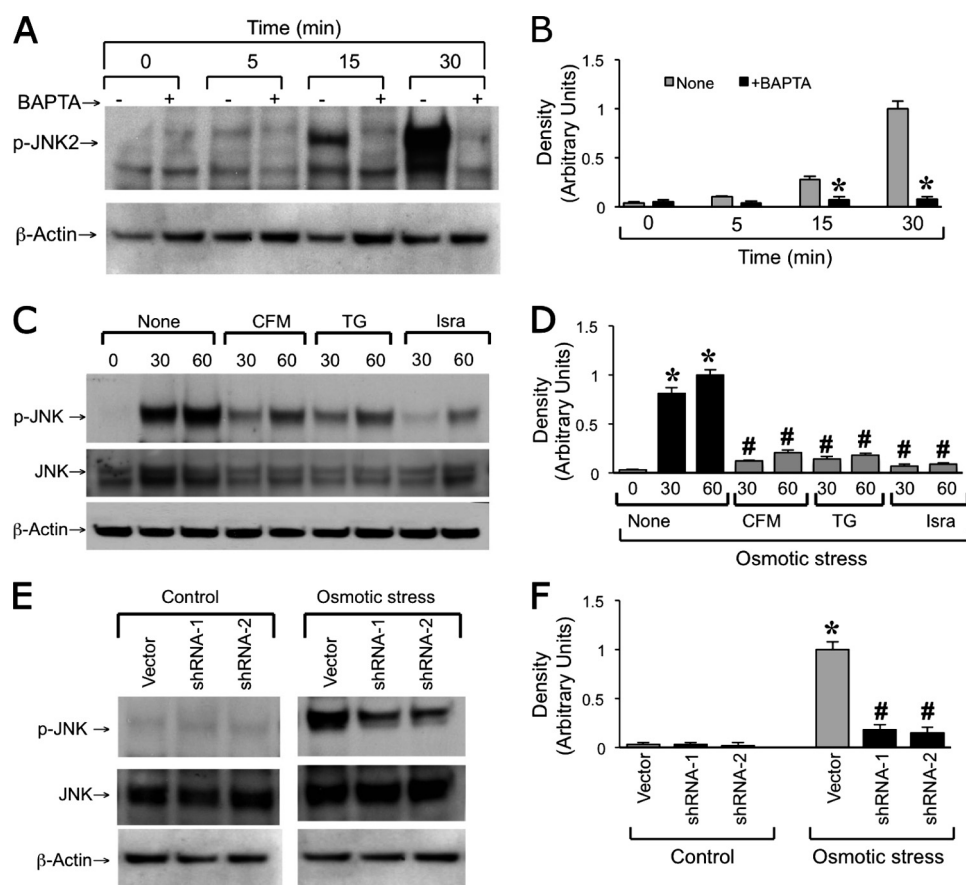


FIGURE 5. Intracellular calcium mediates osmotic stress-induced JNK2 activation. *A* and *B*, Caco-2 cell monolayers were pretreated with or without BAPTA-AM for 30 min prior to osmotic stress. At varying times protein extracts were immunoblotted for phospho-JNK (*p*-JNK). Band densities were evaluated and the values are mean \pm S.E. ($n = 3$). Asterisks indicate the values that are significantly ($p < 0.05$) different from the corresponding value for the control group (None). *C* and *D*, osmotic stress was induced in cell monolayers pretreated with or without thapsigargin (TG) or isradipine (Isra) or incubated with CFM. Protein extracts at varying times were immunoblotted for *p*-JNK and total JNK. Band densities were evaluated and the values are mean \pm S.E. ($n = 3$). Asterisks indicate the values that are significantly ($p < 0.05$) different from the corresponding value for the OS group, and # indicates that values that are significantly different from the corresponding value for the control group (0 min), and # indicates that values that are significantly different from corresponding value for the vector group.

induced increase in *p*-JNK2 was abrogated by pretreatment of cell monolayers with BAPTA-AM (Fig. 5*A*). The osmotic stress-induced increase in *p*-JNK2 was also significantly attenuated by pretreatment of cells with thapsigargin or isradipine or by the removal of extracellular Ca^{2+} from the apical buffer (Fig. 5, *C* and *D*). The osmotic stress-induced increase in the level of *p*-JNK was also attenuated by shRNA-mediated knockdown of $\text{Ca}_v1.3$ (Fig. 5, *E* and *F*).

JNK-mediated c-Src Activation Is Involved in Osmotic Stress-induced Tight Junction Disruption—Previous studies indicated that tyrosine kinases, especially c-Src, play an important role in tight junction disruption by hydrogen peroxide (22) or acetaldehyde (23). In the present study, we evaluated the effect of genistein (a broad range tyrosine kinase inhibitor) and PP2 (Src kinase selective inhibitor) on osmotic stress-induced barrier dysfunction. Both genistein (Fig. 6*A*) and PP2 (Fig. 6*B*) significantly attenuated the osmotic stress-induced increase in inulin permeability. Genistein (Fig. 6*C*) and PP2 (Fig. 6*D*) also prevented osmotic stress-induced redistribution of occludin and ZO-1 from the intercellular junctions. Genistein or PP2 by themselves produced no sig-

nificant effect on inulin permeability or distribution of tight junction proteins.

c-Src is well established to play a role in tyrosine phosphorylation of tight junction proteins and disruption of tight junctions (22). In the present study, we evaluated the role of c-Src activation in osmotic stress-induced tight junction disruption. Osmotic stress induced a transient increase in the level of c-Src(pY418), the activated c-Src (Fig. 7*A*). Osmotic stress-induced elevation of c-Src(pY418) was attenuated by SP600125 (JNK inhibitor) and PP2 (Src kinase inhibitor). Osmotic stress-induced elevation of c-Src(pY418) was also attenuated by removal of extracellular Ca^{2+} or pretreatment of cells with BAPTA-AM or isradipine (Fig. 7*B*). Transfection of Caco-2 cells with c-Src-specific siRNA reduced the level of c-Src (Fig. 7*C*) and attenuated the osmotic stress-induced increase in inulin permeability (Fig. 7*D*). Knockdown of c-SRC also prevented osmotic stress-induced redistribution of occludin and ZO-1 from the intercellular junctions (Fig. 7*E*). Transfection of Caco-2 cells with c-Yes-specific siRNA reduced the level of c-Yes without altering the c-Src level (Fig. 7*F*), but failed to influence the osmotic stress-induced increase in inulin permeability (Fig. 7*G*).

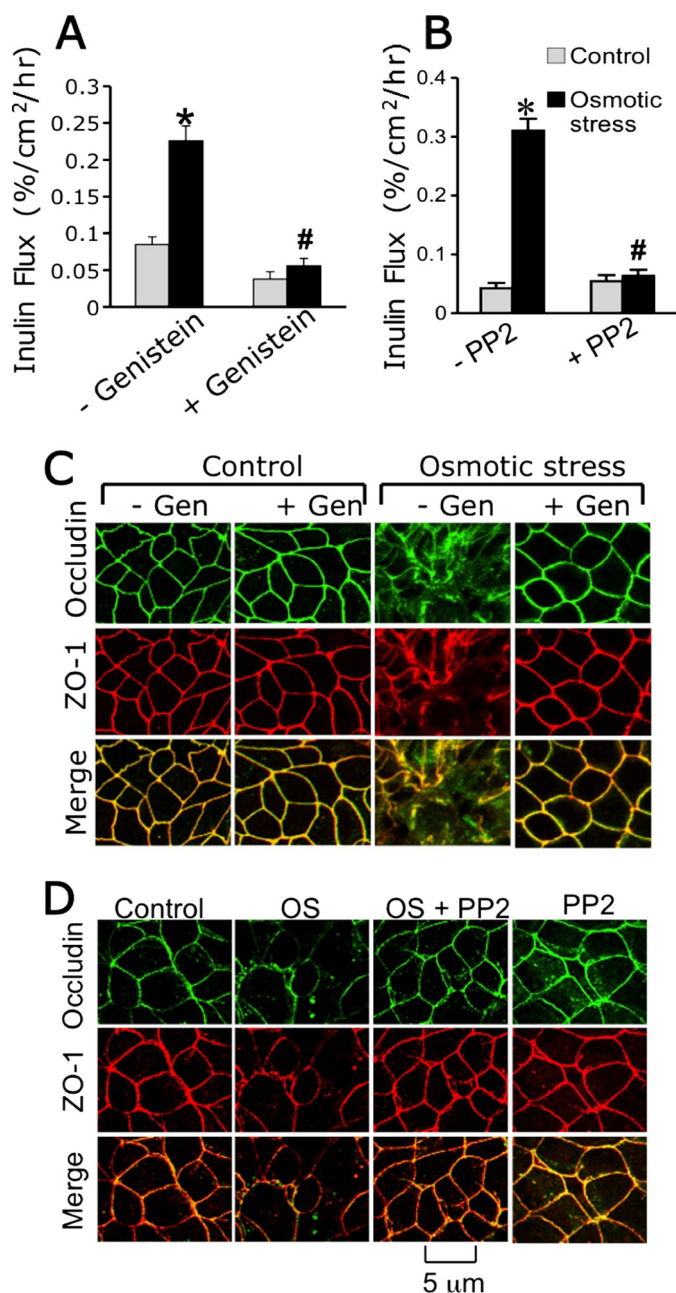


FIGURE 6. Osmotic stress disrupts tight junctions by a tyrosine kinase-dependent mechanism. *A* and *B*, Caco-2 cell monolayers were pretreated with or without genistein (*A*) or PP2 (*B*) for 30 min and osmotic stress was induced as described under "Experimental Procedures." Inulin flux was measured at 1 h after osmotic stress. Values are mean \pm S.E. ($n = 6$). Asterisks indicate the values that are significantly ($p < 0.05$) different from the corresponding control values, and # indicates the values that are different ($p < 0.05$) from the corresponding values for OS without the inhibitor group. *C* and *D*, cell monolayers pretreated with genistein (*C*) or PP2 (*D*) were fixed at 1 h after OS and stained for occludin and ZO-1 by the immunofluorescence method.

Osmotic Stress Induces Tyrosine Phosphorylation of Occludin and ZO-1 by Ca^{2+} , JNK, and Src Kinase-dependent Mechanism—Previous studies showed that tyrosine phosphorylation of tight junction proteins is a key mechanism involved in oxidative stress-induced tight junction disruption and barrier dysfunction (10, 11). Therefore, we examined the effect of osmotic stress on tyrosine phosphorylation of occludin and ZO-1. Osmotic stress induced a robust increase in the level of tyro-

sine-phosphorylated occludin (Fig. 8, *A* and *C*). Osmotic stress-induced occludin phosphorylation was abolished by pretreatment of cells with SP600125. A similar effect of osmotic stress on tyrosine phosphorylation of ZO-1 was observed, however, ZO-1 phosphorylation was weak. Our recent study indicated that JNK2 activity is high in underdifferentiated 4-day-old cell monolayers and knockdown of *JNK* by specific antisense oligonucleotides (AS-Jnk1 and AS-Jnk2) significantly enhanced tight junction integrity in Caco-2 cell monolayers (6). The present study shows that high levels of tyrosine-phosphorylated occludin and ZO-1 were detected in 4-day-old missense oligo-transfected cells (Fig. 8, *B* and *D*). The levels of tyrosine-phosphorylated occludin and ZO-1 were significantly low in cells transfected with AS-Jnk2 and AS-Jnk1. AS-Jnk2 was more effective than AS-Jnk1 in reducing tyrosine phosphorylation of occludin and ZO-1. Furthermore, osmotic stress-induced tyrosine phosphorylation of occludin was attenuated also by pretreatment of cells with BAPTA-AM (Fig. 8*E*) or PP2 (Fig. 8*F*).

DISCUSSION

A significant body of evidence indicates that stress is associated with the pathogenesis of many diseases. One of the major targets of stress-induced tissue injury is the gastrointestinal tract. Our recent study indicated that osmotic stress disrupts the intestinal epithelial tight junctions and induces barrier dysfunction by a JNK2-dependent mechanism. The present study shows that an initial signal triggered by osmotic stress is a rise in $[Ca^{2+}]_i$. The study provides evidence that osmotic stress-induced elevation of $[Ca^{2+}]_i$ involves both $Ca_v1.3$ -mediated Ca^{2+} influx and IP_3 receptor-gated release of store-operated Ca^{2+} . The evidence also demonstrates that $[Ca^{2+}]_i$ mediates stress-induced JNK2 activation and that JNK-mediated c-Src activation and tyrosine phosphorylation of tight junction proteins are the downstream mechanisms to JNK activation leading to tight junction disruption and barrier dysfunction.

A rapid increase in $[Ca^{2+}]_i$, abrogation of osmotic stress-induced tight junction disruption, and barrier dysfunction by BAPTA demonstrate that intracellular $[Ca^{2+}]_i$ plays a crucial role in the osmotic stress-induced tight junction disruption. Although the role of extracellular calcium in formation of adherens junction and maintenance of tight junction integrity is a well established fact, information on the role of $[Ca^{2+}]_i$ in tight junction regulation is sparse. A few studies have indicated that $[Ca^{2+}]_i$ is required for the assembly of tight junctions (14) and for EGF-mediated preservation of tight junctions in acetaldehyde-treated cell monolayers (24). On the other hand, activation of basolateral TRPV4 channel leads to disruption of barrier function in a mammary epithelial cell line (25), and ER calcium release is associated with barrier disruption by ethanol in brain endothelial cells (26) and bacterial infection in Caco-2 cells (27).

A partial reduction of osmotic stress-induced increase in $[Ca^{2+}]_i$ by removal of extracellular calcium indicates that calcium influx from the extracellular source is involved in this response. Removal of extracellular calcium also attenuates osmotic stress-induced tight junction disruption and barrier dysfunction. Interestingly, removal of extracellular calcium from only the apical buffer was sufficient to attenuate osmotic

Tight Junction Regulation by Intracellular Calcium

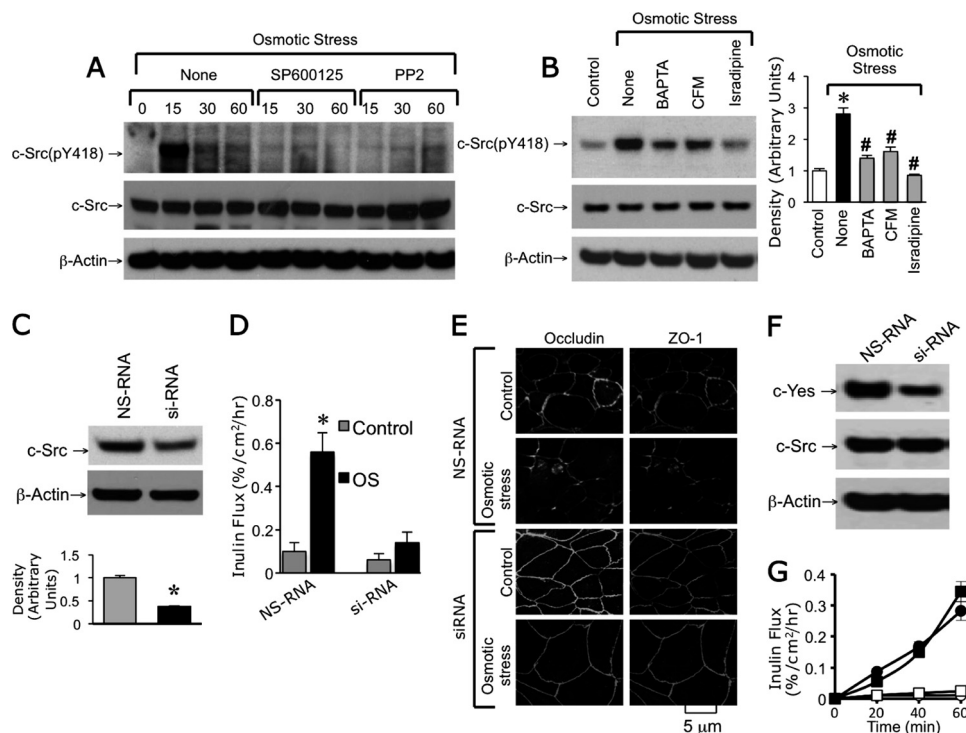


FIGURE 7. Osmotic stress activates c-Src by an intracellular calcium and JNK-dependent mechanism. *A*, Caco-2 cell monolayers were pretreated with or without SP600125 or PP2 for 30 min prior to osmotic stress. At varying times protein extracts were immunoblotted for c-Src(pY418) and total c-Src. *B*, OS was induced in cell monolayers pretreated with or without BAPTA-AM or isradipine (*Isra*) or incubated with CFM. Protein extracts at 30 min after osmotic stress were immunoblotted for Src(pY418) and total c-Src. Asterisks indicate the band density values that are significantly ($p < 0.05$) different from the corresponding value for the control group, and # indicates that values that are significantly different from the corresponding value for "None" in the OS group. *C*, proteins extracted from Caco-2 cells transfected with nonspecific RNA (NS-RNA) or c-Src siRNA were immunoblotted for c-Src and β -actin. Asterisks indicate the band density value that is significantly ($p < 0.05$) different from the corresponding value for the NS-RNA group (gray bar). *D*, Caco-2 cell monolayers transfected with NS-RNA or c-Src siRNA were exposed to osmotic stress for 1 h. Inulin permeability was measured. Values are mean \pm S.E. ($n = 6$). Asterisks indicate the values that are significantly ($p < 0.05$) different from the corresponding control values. # indicates values that are significantly different from the corresponding value for the NS-RNA group. *E*, untreated and osmotic stress-treated cell monolayers were fixed and stained for occludin and ZO-1. *F*, proteins extracted from Caco-2 cells transfected with nonspecific RNA or c-Yes siRNA were immunoblotted for c-Src and β -actin. *G*, Caco-2 cell monolayers transfected with NS-RNA or c-Yes siRNA were exposed to osmotic stress for 1 h. Inulin permeability was measured. Values are mean \pm S.E. ($n = 6$).

stress-induced tight junction disruption. This observation indicates that calcium influx via an apical calcium channel is involved in osmotic stress-induced tight junction disruption. Removal of calcium from the basal medium exacerbated the effect of osmotic stress on tight junction integrity, which is likely mediated by destabilization of adherens junction that is located just basal to tight junctions.

The observation that Ca^{2+} influx from the apical medium is involved in osmotic stress-induced tight junction disruption raised the question about what specific Ca^{2+} channel is involved in osmotic stress-induced Ca^{2+} influx and tight junction disruption. Attenuation of an osmotic stress-induced increase in Ca^{2+} and tight junction disruption by diltiazem and isradipine indicated that the L-type voltage-gated Ca^{2+} channel is involved in osmotic stress-induced tight junction disruption. Several types of voltage-gated Ca^{2+} channels have been described in the apical membrane of intestinal epithelial cells (19). $\text{Ca}_v1.3$, is a major voltage-gated Ca^{2+} channel in the intestinal epithelium. $\text{Ca}_v1.3$ is involved not only in Ca^{2+} absorption (19), but also in Ca^{2+} signaling leading to myosin light chain kinase activation (28). Our present study demonstrates that knockdown of $\text{Ca}_v1.3$ significantly reduces the osmotic stress-induced increase in Ca^{2+} and abrogates osmotic stress-induced tight junction disruption and barrier dysfunction. These results

demonstrate that $\text{Ca}_v1.3$ plays a crucial role in osmotic stress-induced Ca^{2+} influx and tight junction disruption in the intestinal epithelium.

A partial reduction of osmotic stress-induced Ca^{2+} increase by thapsigargin indicates that ER Ca^{2+} release also contributes to a osmotic stress-induced increase in $[\text{Ca}^{2+}]_i$. A significant attenuation of osmotic stress-induced tight junction disruption and barrier dysfunction by thapsigargin demonstrates that ER Ca^{2+} release is required for osmotic stress-induced tight junction disruption. IP_3 receptor activation is a major mechanism involved in ER Ca^{2+} release (29). A significant attenuation of osmotic stress-induced tight junction disruption by xestospingon-C, a selective antagonist of IP_3 receptor, suggests that IP_3 receptors are involved in a osmotic stress-induced rise in $[\text{Ca}^{2+}]_i$ and disruption of tight junctions. Hence, both extracellular Ca^{2+} influx and ER Ca^{2+} release are involved in osmotic stress-induced increase in $[\text{Ca}^{2+}]_i$ and tight junction disruption (Fig. 9). These findings raise a question of whether the two sources of Ca^{2+} contribute to the same pool of $[\text{Ca}^{2+}]_i$ in osmotic stress-treated cells or form two different $[\text{Ca}^{2+}]_i$ pools leading to activation of different downstream signaling pathways. The answer to this question is not clear at this time. It is possible that a high level of Ca^{2+} achieved by multiple sources of Ca^{2+} is required to reach a threshold that trigger down-

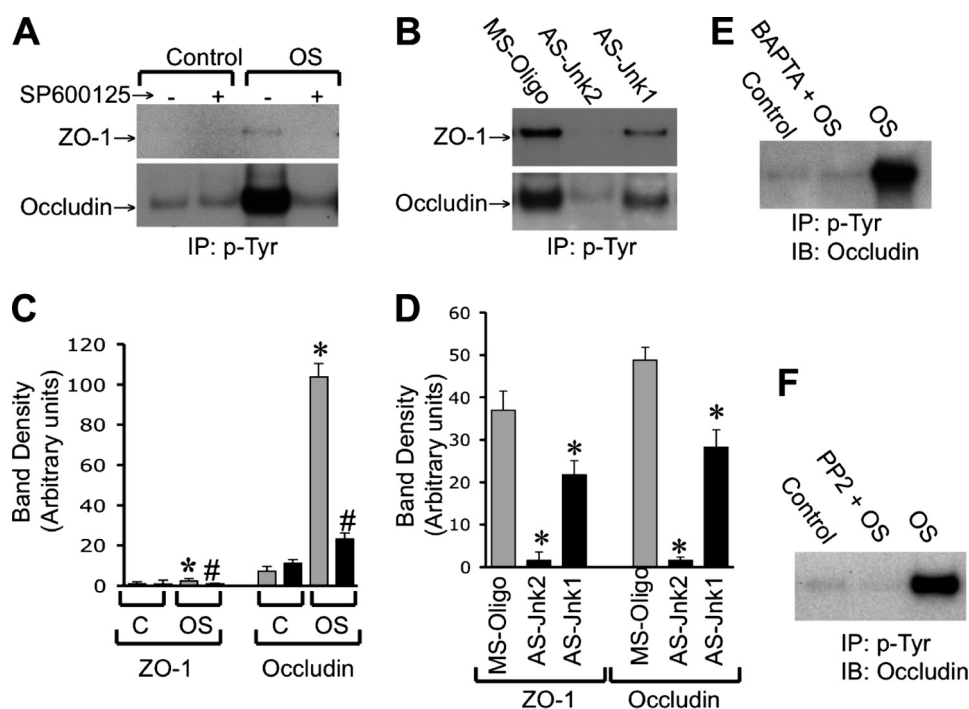


FIGURE 8. Osmotic stress induces tyrosine phosphorylation of occludin and ZO-1 by a calcium-, JNK-, and c-Src-dependent mechanism. *A*, Caco-2 cell monolayers (14 days old, differentiated) were incubated with or without OS for 1 h in the presence or absence of SP600125. Phosphotyrosine was immunoprecipitated from proteins extracted under denaturing conditions and the immunocomplexes were immunoblotted for occludin and ZO-1. *B*, phosphotyrosine immunoprecipitated from cells transfected with different oligos (on day 4 post transfection) were immunoblotted for occludin and ZO-1. *C* and *D*, densitometric analysis of bands in blots related to experiments described in panels *A* (*C*) and *B* (*D*), respectively. Values are mean \pm S.E. ($n = 3$). Asterisks indicate the values that are significantly ($p < 0.05$) different from the corresponding control values or values for MS oligo-transfected cells. # indicates the values that are significantly ($p < 0.05$) different from the corresponding values for the OS group without SP600125. *E* and *F*, phosphotyrosine was immunoprecipitated from proteins extracted from cell monolayers with osmotic stress in the presence or absence of BAPTA (*E*) or PP2 (*F*) and immunoblotted for occludin.

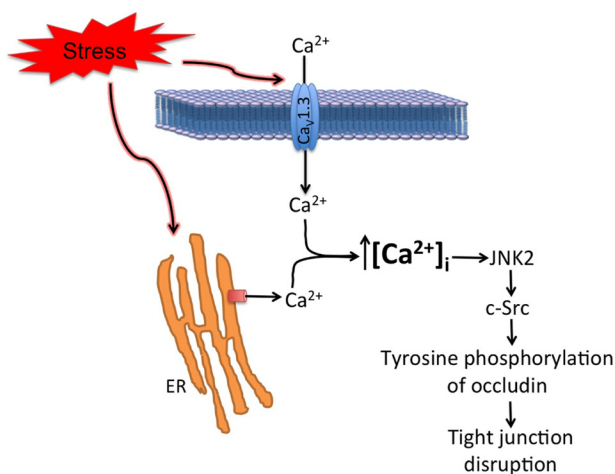


FIGURE 9. Schematic outline of mechanisms associated with osmotic stress-induced tight junction disruption. Results of this study are summarized. The initial signal appears to be an increase in intracellular calcium caused by both influx through the apical calcium channel, $Ca_v1.3$, and intracellular release of ER calcium by IP_3R -mediated mechanism. Rise in intracellular calcium mediates activation of JNK, which in turn activates c-Src leading to tyrosine phosphorylation of tight junction proteins and disruption of tight junctions.

stream signals leading to JNK activation and tight junction disruption.

JNK, originally known as stress-activated protein kinase is activated in cells by various types of stress (30). Our recent study demonstrated that osmotic stress-induced tight junction disruption and barrier dysfunction in the intestinal epithelium

is mediated by JNK2 (6). Knockdown of *JNK* enhances tight junction integrity and attenuates osmotic stress-induced tight junction disruption in Caco-2 cell monolayers (6). Osmotic stress-induced tight junction disruption was absent in ileum of *JNK2* knock-out mice. Additionally, cold-restraint stress-induced tight junction disruption in rat ileum was attenuated by the administration of a JNK-selective inhibitor, SP600125. The observation that $[Ca^{2+}]_i$ plays a role in osmotic stress-induced tight junction disruption raised the question whether JNK activation and rise in $[Ca^{2+}]_i$ are interdependent. The time course studies indicated that the increase in $[Ca^{2+}]_i$ reached a peak within 5 min after administration of the hyperosmotic mannitol. On the other hand, JNK activation required about 15 min with the peak level achieved at 30 min. Therefore, we reasoned that $[Ca^{2+}]_i$ mediates osmotic stress-induced JNK activation. Osmotic stress-induced JNK activation was indeed attenuated by extracellular Ca^{2+} depletion or treatment of cells with thapsigargin, diltiazem, or isradipine, indicating that both Ca^{2+} influx and ER Ca^{2+} are required for osmotic stress-induced JNK activation. This also provides supporting evidence to the speculation that the two sources of Ca^{2+} are required to maintain $[Ca^{2+}]_i$ at a concentration high enough to induce JNK activation. The mechanism associated with Ca^{2+} -induced JNK activation is unknown. It is likely that $[Ca^{2+}]_i$ activates MKK7, which in turn activates JNK2.

A significant body of evidence indicates that c-Src activity causes tight junction disruption in different epithelia including Caco-2 cell monolayers (22). c-Src regulates phosphorylation of

Tight Junction Regulation by Intracellular Calcium

occludin and other tight junction and adherens junction proteins leading to dissociation of protein-protein interactions and disruption of tight junctions (22). In the present study, we examined the potential role of the Src kinase in osmotic stress-induced tight junction disruption. Attenuation of osmotic stress-induced tight junction disruption and barrier dysfunction by genistein and PP2 displayed a clear indication of the role of Src kinase in osmotic stress-induced tight junction disruption. The present study shows that osmotic stress causes a rapid and transient increase in the level of c-Src(pY418) indicating the activation of c-Src by osmotic stress. Attenuation of osmotic stress-induced c-Src activation by SP600125 indicated that Src activation is downstream to JNK activation. Activation of c-Src by osmotic stress was also attenuated by BAPTA, extracellular Ca^{2+} depletion, or isradipine, demonstrating that Ca^{2+} -mediated JNK activation is responsible for c-Src activation. The role of c-Src in osmotic stress-induced tight junction disruption was confirmed by knockdown of c-SRC using specific siRNA. Osmotic stress-induced increase in inulin permeability and redistribution of occludin and ZO-1 were effectively attenuated by c-SRC knockdown. Interestingly, specific knockdown of c-YES did not influence osmotic stress-induced paracellular permeability.

Previous studies demonstrated that c-Src activation leads to phosphorylation of many tight junction and adherens junction proteins. Phosphorylation of occludin on specific tyrosine residues results in loss of its interaction with ZO-1 and enhanced susceptibility to hydrogen peroxide-induced tight junction disruption in Caco-2 and Madin-Darby canine kidney cell monolayers (10, 11). Similarly, Src-mediated tyrosine phosphorylation of β -catenin on specific tyrosine residues attenuates its interaction with E-cadherin (31). The present study examined the effect of osmotic stress on tyrosine phosphorylation of occludin and ZO-1. Tyrosine phosphorylation of ZO-1 was weak, whereas osmotic stress induced a robust increase in tyrosine phosphorylation of occludin. Osmotic stress-induced tyrosine phosphorylation of occludin was abrogated by SP600125, indicating the role of JNK activity in osmotic stress-induced occludin tyrosine phosphorylation. The role of JNK in occludin phosphorylation was further supported by a reduced level of basal occludin phosphorylation in cells transfected with JNK-specific antisense oligonucleotides. Osmotic stress-induced occludin tyrosine phosphorylation was also attenuated by pretreatment of cell monolayers with BAPTA or PP2. These studies indicate that tyrosine phosphorylation of occludin is mediated by Ca^{2+} -induced JNK activation and subsequent Src activation. It is likely that tyrosine phosphorylation of occludin results in loss of interaction between occludin and ZO-1. The mechanism of JNK-mediated c-Src activation is unclear at this time. But, evidence indicates that c-Src activity can be regulated by Ser/Thr phosphorylation (32), allowing us to speculate that JNK may directly phosphorylate c-Src.

Our previous study demonstrated that occludin is phosphorylated by c-Src (10). Both mass spectrometric analysis and point mutation studies indicated that only Tyr-398 and Tyr-402 are phosphorylated by c-Src. In the present study, the data show that osmotic stress-induced occludin Tyr phosphorylation is completely attenuated by Src kinase inhibitor, suggesting

that Tyr-398 and Tyr-402 are phosphorylated during OS-induced TJ disruption.

A question that arises in this study is whether $\text{Ca}_v1.3$ -mediated Ca^{2+} influx regulates the stored calcium level, and therefore ER release of Ca^{2+} . An answer to this question is unclear at this point. Our data show that removal of extracellular calcium or depletion of stored calcium by thapsigargin only partially prevents a OS-induced rise in $[\text{Ca}^{2+}]_i$. However, the voltage-gated Ca^{2+} channel blocker, $\text{Ca}_v1.3$ knockdown, and xestospingon-C all effectively attenuate OS-induced TJ disruption. Based on these data we speculate that a threshold level of $[\text{Ca}^{2+}]_i$ is required to be achieved to induce TJ disruption. Therefore, reduction of the OS-induced rise in $[\text{Ca}^{2+}]_i$ to half either by calcium-free medium or thapsigargin attenuates OS-induced TJ disruption.

In summary, this study demonstrates that osmotic stress induces a rapid increase in $[\text{Ca}^{2+}]_i$ via $\text{Ca}_v1.3$ -mediated extracellular Ca^{2+} influx and IP_3 receptor-mediated ER Ca^{2+} release. This increase in $[\text{Ca}^{2+}]_i$ caused a rapid activation of JNK2 and disruption of tight junction. Furthermore, c-Src activation and tyrosine phosphorylation of occludin mediates the JNK2 effect on tight junction integrity.

REFERENCES

1. Mawdsley, J. E., and Rampton, D. S. (2005) *Gut* **54**, 1481–1491
2. Madara, J. L. (1983) *J. Cell Biol.* **97**, 125–136
3. Cheromcha, D. P., and Hyman, P. E. (1988) *Dig. Dis. Sci.* **33**, 78S–84S
4. Schilli, R., Breuer, R. I., Klein, F., Dunn, K., Gnaedinger, A., Bernstein, J., Paige, M., and Kaufman, M. (1982) *Gut* **23**, 326–332
5. Vernia, P., Gnaedinger, A., Hauck, W., and Breuer, R. I. (1988) *Dig. Dis. Sci.* **33**, 1353–1358
6. Samak, G., Suzuki, T., Bhargava, A., and Rao, R. K. (2010) *Am. J. Physiol. Gastrointest. Liver Physiol.* **299**, G572–584
7. Van Itallie, C. M., and Anderson, J. M. (2004) *Physiology* **19**, 331–338
8. Rao, R. (2008) *Front. Biosci.* **13**, 7210–7226
9. Balda, M. S., and Matter, K. (2008) *J. Cell Sci.* **121**, 3677–3682
10. Elias, B. C., Suzuki, T., Seth, A., Giorgianni, F., Kale, G., Shen, L., Turner, J. R., Naren, A., Desiderio, D. M., and Rao, R. (2009) *J. Biol. Chem.* **284**, 1559–1569
11. Kale, G., Naren, A. P., Sheth, P., and Rao, R. K. (2003) *Biochem. Biophys. Res. Commun.* **302**, 324–329
12. Seth, A., Sheth, P., Elias, B. C., and Rao, R. (2007) *J. Biol. Chem.* **282**, 11487–11498
13. Balda, M. S., González-Mariscal, L., Contreras, R. G., Macias-Silva, M., Torres-Marquez, M. E., García-Sáinz, J. A., and Cerejido, M. (1991) *J. Membr. Biol.* **122**, 193–202
14. Brown, R. C., and Davis, T. P. (2002) *Stroke* **33**, 1706–1711
15. Ma, T. Y., Tran, D., Hoa, N., Nguyen, D., Merryfield, M., and Tarnawski, A. (2000) *Microsc. Res. Tech.* **51**, 156–168
16. Mandel, L. J., Bacallao, R., and Zampighi, G. (1993) *Nature* **361**, 552–555
17. Ye, J., Tsukamoto, T., Sun, A., and Nigam, S. K. (1999) *Am. J. Physiol. Renal Physiol.* **277**, F524–F532
18. Stuart, R. O., Sun, A., Bush, K. T., and Nigam, S. K. (1996) *J. Biol. Chem.* **271**, 13636–13641
19. Nakkrasae, L. I., Thongon, N., Thongbunchoo, J., Krishnamra, N., and Charoenphandhu, N. (2010) *J. Physiol. Sci.* **60**, 9–17
20. Suzuki, T., Elias, B. C., Seth, A., Shen, L., Turner, J. R., Giorgianni, F., Desiderio, D., Guntaka, R., and Rao, R. (2009) *Proc. Natl. Acad. Sci. U.S.A.* **106**, 61–66
21. Rao, R. K., Basuroy, S., Rao, V. U., Karnaky, Jr., K. J., and Gupta, A. (2002) *Biochem. J.* **368**, 471–481
22. Basuroy, S., Sheth, P., Kuppuswamy, D., Balasubramanian, S., Ray, R. M., and Rao, R. K. (2003) *J. Biol. Chem.* **278**, 11916–11924

23. Atkinson, K. J., and Rao, R. K. (2001) *Am. J. Physiol. Gastrointest. Liver Physiol.* **280**, G1280–G1288
24. Suzuki, T., Seth, A., and Rao, R. (2008) *J. Biol. Chem.* **283**, 3574–3583
25. Reiter, B., Kraft, R., Günzel, D., Zeissig, S., Schulzke, J. D., Fromm, M., and Harteneck, C. (2006) *FASEB J.* **20**, 1802–1812
26. Haorah, J., Knipe, B., Gorantla, S., Zheng, J., and Persidsky, Y. (2007) *J. Neurochem.* **100**, 324–336
27. Vikström, E., Bui, L., Konradsson, P., and Magnusson, K. E. (2010) *Eur. J. Cell Biol.* **89**, 584–597
28. Mace, O. J., Morgan, E. L., Affleck, J. A., Lister, N., and Kellett, G. L. (2007) *J. Physiol.* **580**, 605–616
29. Berridge, M. J., Bootman, M. D., and Roderick, H. L. (2003) *Nat. Rev. Mol. Cell Biol.* **4**, 517–529
30. Lin, A. (2003) *Bioessays* **25**, 17–24
31. Sheth, P., Seth, A., Atkinson, K. J., Gheyi, T., Kale, G., Giorgianni, F., Desiderio, D. M., Li, C., Naren, A., and Rao, R. (2007) *Biochem. J.* **402**, 291–300
32. Chackalaparampil, I., and Shalloway, D. (1988) *Cell* **52**, 801–810